

A one-dimensional model of surface growth.

RA, EP, GT
April 27, 2019

File:Growth_BodyForce.tex in
Folder: Paper-body force/Puntel Paper/Desktop

0.1 Problem.

These notes are quite rough and needs fixing. I'm sending it now so you can get a feel for it.

The system we have in mind is illustrated schematically in Figure 1, though we use a purely one-dimensional model to study it. **The key feature of this model is that we assume the diffusion of monomers through the solid applies a (known constant) body force on the solid.** This leads to a compressive stress field within the solid, with the maximum compression occurring at the association end. The magnitude of the compressive stress at each particle increases as the body grows. The “loading” in this problem is the remote chemical potential μ_∞ and the response of the sytem for various ranges of the chemical potential is examined.

We calculate two critical values of the chemical potential μ_{cr} and μ_{CR} ($> \mu_{cr}$). For $\mu_\infty < \mu_{cr}$ the body will not grow at all, or a previously grown body will shrink until it disappears fully. For $\mu_\infty > \mu_{CR}$ the body will grow indefinitely. For $\mu_{cr} < \mu_\infty < \mu_{CR}$ the body will grow until it reaches a certain steady state where the rate of association exactly balances the rate of dissociation and so the size of the body in physical space no longer changes (though association/dissociation continues to occur).

In physical space, the solid body – a “polymer” – is identified with the slab-like region $y_0 \leq y \leq y_1(t)$ (with $-\infty < y_2, y_3 < \infty$). There is a reservoir of (unbound) free particles – “monomers” – in the region $y > y_1(t)$ to the right of the body which is at a chemical potential μ_∞ . The monomers diffuse through the solid in the negative y -direction until they reach the rigid impermeable wall at $y = 0$. Here, they bind to the polymer and thus the body continually undergoes “association” (polymerization or accretion) at $y = 0$. New solid material is continually formed in this way, one layer at a time, with each new layer pushing out the previously formed layers. Simultaneously, the body may steadily lose monomers its right-hand face $y = y_1(t)$ by dissociation (depolymerization or ablation) one layer at a time. In the analysis, we permit the body to undergo either association or dissociation at each end, with the energetics of the system determining as to which in fact occurs.

So the force intensity does not depend on the flux, right? Maybe it is only a small change because we would have $b(t)$ constant in space but not in time. --> but it has consequences

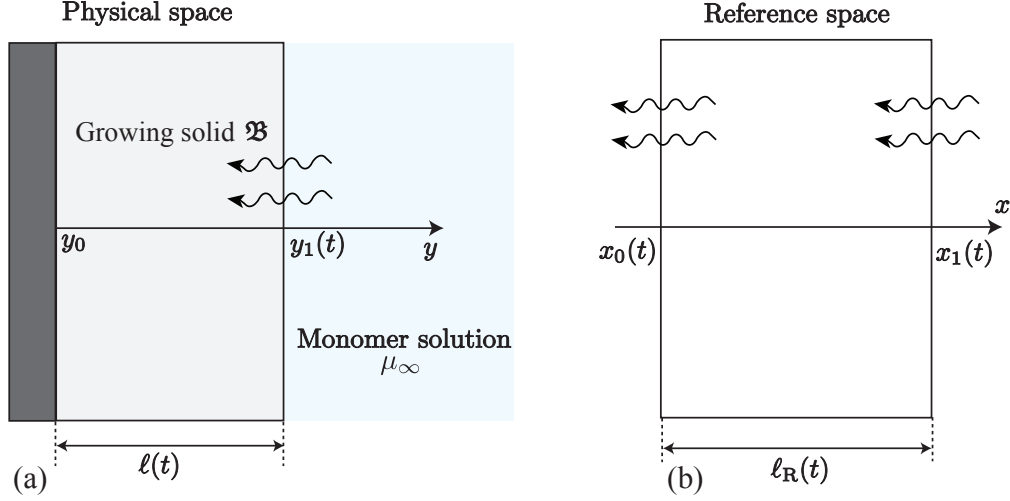


Figure 1: (a) Solid body in physical space with a reservoir of free unbound monomers on its right and a rigid impermeable wall on its left. (b) The solid body in reference space at time t . The respective lengths of the solid in physical and reference space are $\ell(t)$ and $\ell_R(t)$.

0.2 Solid material

The solid material is characterized by its strain energy density function $W(\lambda)$ where λ is the stretch, and the stress σ is related to the stretch through the constitutive relation

$$\sigma = W'(\lambda). \quad (1)$$

It is assumed that $\sigma(\lambda)$ is a monotonically increasing function, and that $\sigma(\lambda) \rightarrow -\infty$ as $\lambda \rightarrow 0^+$ and $\sigma(\lambda) \rightarrow \infty$ as $\lambda \rightarrow \infty$. The stretch can therefore be expressed as a function of stress as

$$\lambda = \widehat{\lambda}(\sigma), \quad (2)$$

where $\widehat{\lambda}(\sigma)$ is defined for $-\infty < \sigma < \infty$. The complementary energy function $\overset{*}{W}(\sigma)$ is the Legendre transform of $W(\lambda)$ and as such is defined by

$$\overset{*}{W} = \sigma\lambda - W, \quad \text{or more completely by } \overset{*}{W}(\sigma) = \sigma\widehat{\lambda}(\sigma) - W(\widehat{\lambda}(\sigma)). \quad (3)$$

It can be readily verified that

$$\lambda = \overset{*}{W}'(\sigma). \quad (4)$$

The complementary energy function is assumed to have the following properties:

$$\overset{*}{W}(0) = 0, \quad \overset{*}{W}'(0) = 1, \quad (5)$$

$$00414\text{-eq4a}\} \quad \overset{*}{W}'(\sigma) > 0 \quad \text{for all } \sigma \quad (6)$$

$$00414\text{-eq4b}\} \quad \overset{*}{W}''(\sigma) = \widehat{\lambda}'(\sigma) > 0 \quad \text{for all } \sigma \quad (7)$$

$$190414\text{-eq6}\} \quad \overset{*}{W}(\sigma) \rightarrow \pm\infty \quad \text{as } \sigma \rightarrow \pm\infty \quad (8)$$

$$190414\text{-eq6}\} \quad \overset{*}{W}'(\sigma) \rightarrow \infty \quad \text{as } \sigma \rightarrow \infty, \quad \overset{*}{W}'(\sigma) \rightarrow 0 \quad \text{as } \sigma \rightarrow -\infty \quad (9)$$

Note in particular that

$$190414\text{-eq5}\} \quad \overset{*}{W}(\sigma) < 0 \quad \text{for } \sigma < 0. \quad (10)$$

Also, W and $\overset{*}{W}$ have the dimension **energy/vol** while σ has the dimension **force/area**.

Example: While we will not need to consider any explicit form of W in this study, when plotting results we shall use the following particular function W . The functions $W(\lambda)$ and $\overset{*}{W}(\sigma)$ below do not have all of the properties listed above (in particular $\overset{*}{W}(\sigma)$ is defined for $-\infty < \sigma < E/2$ rather than for all σ . However they *do* have the properties relevant to compression, i.e. for $\lambda \in (0, 1], \sigma \in (-\infty, 0)$, and compression is all we encounter in the problem to be studied here. The explicit example is

$$190414\text{-eq7}\} \quad W(\lambda) = \frac{E}{2}(\lambda + \lambda^{-1} - 2) \quad \text{for } \lambda > 0 \quad (11)$$

$$190414\text{-eq8}\} \quad \sigma(\lambda) = W'(\lambda) = \frac{E}{2}(1 - \lambda^{-2}) \quad (12)$$

I want to check
these equations

$$190414\text{-eq9}\} \quad \widehat{\lambda}(\sigma) = \frac{1}{\sqrt{1 - 2\sigma/E}} \quad \text{for } -\infty < \sigma < E/2 \quad (13)$$

$$00414\text{-eq10}\} \quad \overset{*}{W}(\sigma) = E - E\sqrt{1 - 2\sigma/E} \quad \text{for } -\infty < \sigma < E/2 \quad (14)$$

0.3 Mechanics

00414-sec3}

In our one-dimensional model the body is identified in physical space with the slab-like region $y_0 \leq y \leq y_1(t)$, $(-\infty < y_2, y_3 < \infty)$, while its image in reference space is $x_0(t) \leq x \leq x_1(t)$, $(-\infty < x_2, x_3 < \infty)$, see Figure 1. The respective lengths of the body in physical and reference space are

$$00414\text{-eq11}\} \quad \ell(t) = y_1(t) - y_0 \geq 0, \quad \ell_R(t) = x_1(t) - x_0(t) \geq 0. \quad (15)$$

The body undergoes a motion

$$y = y(x, t), \quad \text{for } x_0(t) \leq x \leq x_1(t), \quad t \geq 0, \quad (16)$$

subject to

$$y(x_0(t), t) = y_0, \quad y(x_1(t), t) = y_1(t). \quad (17)$$

The stress $\sigma(x, t)$ obeys the equilibrium equation

$$\text{90414-eq12}\} \quad \frac{\partial \sigma}{\partial x} - b = 0, \quad \text{for } x_0(t) < x < x_1(t) \quad (18)$$

where the constant body force $b > 0$ accounts for the drag force applied on the solid by the monomers diffusing through it in the negative x -direction. It has the dimension **stress/length**. The right-hand face of the body is traction-free and so

$$\text{90414-eq13}\} \quad \sigma_1(t) := \sigma(x_1(t), t) = 0 \quad \text{for } t \geq 0. \quad (19)$$

Integrating (18) subject to the boundary condition (19) gives the stress field in the body to be

$$\text{90414-eq14}\} \quad \sigma(x, t) = -b[x_1(t) - x], \quad \text{for } x_0(t) < x < x_1(t). \quad (20)$$

The stress is therefore compressive at each point x , becoming increasingly more compressive as x decreases from $x_1(t)$ to $x_0(t)$. The stress at the left-hand face of the slab where it is in contact with the impermeable wall is

$$\text{90414-eq15}\} \quad \sigma_0(t) := \sigma(x_0(t), t) = -b(x_1(t) - x_0(t)) \stackrel{(15)}{=} -b\ell_R(t) \leq 0. \quad (21)$$

The constitutive relation $(4)_2$ relates the stretch λ to the stress σ through $\lambda = \overset{*}{W}'(\sigma)$. Since the stretch $\lambda = \partial y / \partial x$ and the stress is given by (20), we therefore have

$$\text{90414-eq16}\} \quad \frac{\partial y}{\partial x} = \overset{*}{W}'(bx - bx_1). \quad (22)$$

Integrating this and using $y(x_1(t), t) = y_1(t)$ gives

$$\text{90414-eq17}\} \quad y(x, t) = \frac{1}{b} \overset{*}{W}(bx - bx_1(t)) + y_1(t), \quad \text{for } x_0(t) \leq x \leq x_1(t). \quad (23)$$

Since $y(x_0(t), t) = y_0$ at the left-hand end of the body, it follows that

$$\text{90414-eq18}\} \quad y_1(t) = y_0 - \frac{1}{b} \overset{*}{W}(bx_0(t) - bx_1(t)). \quad (24)$$

Equation (24) shows that the lengths $\ell(t) = y_1(t) - y_0$ and $\ell_R(t) = x_1(t) - x_0(t)$ of the body in physical and referential space are related by

$$\text{90414-eq19}\} \quad \ell = -\frac{1}{b} \overset{*}{W}(-b\ell_R). \quad (25)$$

Since the stress at the left-hand face $\sigma_0(t) = -b\ell_R$, see (21), we conclude that

$$\ell(t) = -\frac{1}{b} \overset{*}{W}(\sigma_0(t)). \quad (26)$$

Finally it will be useful to note by differentiating (25) that

$$\dot{\ell} = \dot{W}'(-b\ell_R)\dot{\ell}_R. \quad (27)$$

Thus, since $\dot{W}' > 0$ by (6)₁, it follows that

$$\dot{\ell} = 0 \quad \text{if and only if} \quad \dot{\ell}_R = 0. \quad (28)$$

In summary, if we know $x_0(t)$ and $x_1(t)$, the motion $y(x, t)$ of the body is given by (23), the stress field is given by (20), and the lengths of the body in reference and physical space are given by (20)₂ and (25). The position $y_1(t)$ of the right-hand face of the body is given by (24), the left-hand position y_0 being taken to be prescribed. At this stage we are yet to determine $x_0(t)$ and $x_1(t)$.

0.4 Diffusion

Let $h(y, t)$ denote the monomer flux in the positive y -direction (nnn check this nnn) (dimension mass per unit area per unit time) and let $\mu(y, t)$ be the chemical potential of the *unbound* free monomers (dimension energy/mass). They are related by Fick's law

$$h = -D \frac{\partial \mu}{\partial y}, \quad (29)$$

where the constant parameter $D > 0$ is the diffusion coefficient (dimension mass · time per unit volume). Assuming the diffusion of monomers to be steady we may ignore the time derivative term in the mass balance equation and write

$$\frac{\partial h}{\partial y} = 0, \quad \text{for } y_0 \leq y \leq y_1(t). \quad (30)$$

Substituting (29) into (30) gives $\partial^2 \mu / \partial y^2 = 0$ which upon integration yields

$$\mu(y, t) = \mu_\infty \frac{y - y_0}{y_1(t) - y_0} - \mu_0(t) \frac{y - y_1(t)}{y_1(t) - y_0} \quad \text{for } y_0 < y < y_1(t), \quad (31)$$

where we have required

$$\mu(y_0, t) = \mu_0(t), \quad \mu(y_1(t), t) = \mu_\infty. \quad (32)$$

The chemical potential μ_∞ is the *given* chemical potential in the monomer reservoir on the right-hand side of the body (see Figure 1) and we have used the continuity of the chemical potential to write (32)₂; $\mu_0(t)$ is the as yet unknown chemical potential of the unbound free monomers at the left-hand wall. From (29) and (31) we have the monomer flux to be

$$h(y, t) = -D \frac{\mu_\infty - \mu_0(t)}{y_1(t) - y_0} \quad \text{for } y_0 < y < y_1(t). \quad (33)$$

In summary, if we know $x_0(t)$ and $x_1(t)$, the position $y_1(t)$ of the right-hand face of the body is found from (24), keeping in mind that the left-hand position y_0 is prescribed. Furthermore, if the chemical potential $\mu_0(t)$ at the left-hand end is known then the chemical potential of the free monomer field is given by (31) and the flux of free monomers is given by (33). At this stage we are yet to determine $x_0(t), x_1(t)$ and $\mu_0(t)$.

NNN Inconsistency with direction of h . To the left or the right?

I think the direction of h is correct and it is to the left.

0.5 Coupling mechanics and diffusion.

Let $\rho > 0$ be the mass density of the solid (the monomers bound to the solid) (dimension mass/volume). Since the left-hand boundary in reference space has velocity \dot{x}_0 , the mass of monomers added to the body at x_0 per unit area per unit time is $\rho\dot{x}_0$. The flux of incoming free monomers flowing into this surface through the solid (mass per unit area per unit time) is $h(y_0, t)$. The conservation of mass requires these two quantities to be equal and so we have the coupling condition

$$h(y_0, t) = \rho\dot{x}_0. \quad (34)$$

Substituting (24) into this allows us to solve for the chemical potential $\mu_0(t)$:

$$\mu_0 = \mu_\infty + \frac{\rho}{D} \ell \dot{x}_0 = \mu_\infty - \frac{\rho}{D} \frac{1}{b} \dot{W}^*(-bl_R) \dot{x}_0, \quad (35)$$

where we have also used (15) in getting the first expression and used (25) in getting the second. Having now found $\mu_0(t)$, we are left with determining $x_0(t)$ and $x_1(t)$.

0.6 Driving force and kinetics.

The driving forces associated with growth are shown in Appendix A to be

$$f_0 = \rho(\mu_0 - \bar{\mu}_0) + \dot{W}^*(\sigma_0), \quad (36)$$

f has dimension of energy per volume.

$$f_1 = \rho(\mu_\infty - \bar{\mu}_1) + \dot{W}^*(\sigma_1), \quad (37)$$

at x_0 and x_1 respectively. As above, $\mu_0(t)$ and $\mu_1 = \mu_\infty$ are the chemical potentials of the free unbound monomers at x_0 and x_1 respectively. As for the constant parameters $\bar{\mu}_0$ and $\bar{\mu}_1$, these denote the respective chemical potentials at x_0 and x_1 of the monomers bound to the solid. We shall assume throughout that

$$\bar{\mu}_1 > \bar{\mu}_0. \quad (38)$$

...I am not so sure about this claim

This seems to be consisted with experimental observations, see for example [?, nnn]

The growth velocities at the two ends are

$$90414\text{-eq39}\} \quad V_0 = -\dot{x}_0, \quad V_1 = \dot{x}_1, \quad (39)$$

as can be seen from Figure 1(b). Observe that for both $\alpha = 0$ and $\alpha = 1$, $V_\alpha > 0$ refers to association, while $V_\alpha < 0$ refers to dissociation. Yes, I remark I could have added to the draft of the paper

We assume the growth process to be not far from thermodynamic equilibrium and so take the kinetic law for growth to be linear:

$$90414\text{-eq39}\} \quad B_0 V_0 = f_0, \quad B_1 V_1 = f_1. \quad (40)$$

Here the kinetic rates $B_0 > 0, B_1 > 0$ are positive constant parameters (with dimension mass per unit area per unit time). It will be convenient in what follows to introduce the weighted average chemical potential

$$90414\text{-eq60}\} \quad \bar{\mu}_* := \frac{\bar{\mu}_1 B_0 + \bar{\mu}_0 B_1}{B_0 + B_1}, \quad \bar{\mu}_0 < \bar{\mu}_* < \bar{\mu}_1. \quad (41)$$

Combining (36), (39) and (40) gives $\dot{x}_0 = -\frac{1}{B_0} \frac{\rho(\mu_\infty - \bar{\mu}_0) + \dot{W}^*(-b\ell_R)}{1 - \frac{\rho^2}{bB_0D} \dot{W}^*(-b\ell_R)}$

$$90414\text{-eq41}\} \quad -\dot{x}_0 = \frac{1}{B_0} \left[\rho(\mu_\infty - \bar{\mu}_0) + \dot{W}^*(\sigma_0) \right], \quad (42)$$

from which the chemical potential μ_0 can be eliminated using (35) to get

$$90414\text{-eq43}\} \quad \dot{x}_0 = \dot{x}_0(\ell_R) := X(\ell_R) := \frac{Db/\rho^2}{B_0} \frac{\rho(\mu_\infty - \bar{\mu}_0) + DbB_0/\rho^2}{1 - \frac{\rho^2}{DbB_0} \dot{W}^*(-b\ell_R)} \quad (43)$$

Similarly at the end x_1 , (37), (39) and (40) gives

$$90414\text{-eq44}\} \quad \dot{x}_1 = \frac{1}{B_1} \left[\rho(\mu_\infty - \bar{\mu}_1) + \dot{W}^*(\sigma_1) \right], \quad (44)$$

which can be simplified since the stress σ_1 at $x = x_1$ vanishes and $\dot{W}^*(0) = 0$, thus leading to

$$90414\text{-eq45}\} \quad \dot{x}_1 = \dot{x}_1(\ell_R) := \frac{\rho}{B_1} (\mu_\infty - \bar{\mu}_1). \quad (45)$$

Remark: Observe that \dot{x}_1 , and therefore the growth rate V_1 , is time-independent whenever the remote chemical potential μ_∞ is held constant. Interesting

Now consider the length $\ell_R = x_1 - x_0 \geq 0$ of the body in the reference configuration. From (43) and (45):

$$00414\text{-eq46}\} \quad \dot{\ell}_R = R(\ell_R) := \dot{x}_1(\ell_R) - \dot{x}_0(\ell_R) = \frac{\rho}{B_1}(\mu_\infty - \bar{\mu}_1) - \frac{1}{B_0} \frac{\rho(\mu_\infty - \bar{\mu}_0) + \cancel{DbB_0/\rho^2} \overset{*}{W}(-b\ell_R)}{1 - \frac{g^2}{DbB_0} \overset{*}{W}(-b\ell_R)}. \quad (46)$$

Observe that

$$00414\text{-eq47}\} \quad R(0) = \frac{\rho}{B_1}(\mu_\infty - \bar{\mu}_1) + \frac{\rho}{B_0}(\mu_\infty - \bar{\mu}_0), \quad R(\infty) = \frac{\rho}{B_1}(\mu_\infty - \bar{\mu}_1) + Db/\rho^2, \quad (47)$$

whence we can write (46) as

$$00414\text{-eq48}\} \quad \dot{\ell}_R = R(\ell_R) = R(\infty) + \frac{R(0) - R(\infty)}{1 - \frac{g^2}{DbB_0} \overset{*}{W}(-b\ell_R)}. \quad (48)$$

This is a first-order differential equation for the length $\ell_R(t)$. Keep in mind that $\overset{*}{W} < 0$ at all negative values of its argument and so the denominator in (48) is always strictly positive (and in particular never vanishes).

Remark: Recall that from (25) and (21) that

$$00414\text{-eq68}\} \quad \overset{*}{W}(-b\ell_R) = -b\ell \leq 0 \quad \text{and} \quad \sigma_0 = -b\ell_R \leq 0. \quad (49)$$

0.7 Evolution of the referential length $\ell_R(t)$.

00414-sec8}

The evolution of the referential length $\ell_R(t)$ of the body is given by the solutions of the first order differential equation

$$\dot{\ell}_R = R(\ell_R) \quad (50)$$

where the function $R(\ell_R)$ was defined for all $\ell_R \geq 0$ by (46). Since $\overset{*}{W}'(-b\ell_R) > 0$ it follows from (48) that $R(\ell_R)$ is a monotonically increasing function of ℓ_R in the case $R(0) < R(\infty)$ (Case 1) and a monotonically decreasing function in the case $R(0) > R(\infty)$ (Cases 2a,b,c). The special case $R(0) = R(\infty)$ occurs when

$$\mu_\infty = \bar{\mu}_0 - DbB_0/\rho^3, \quad (51)$$

and in this case the rate at which the length ℓ_R grows has the negative constant value

$$\dot{\ell}_R = \frac{\rho}{B_1}(\bar{\mu}_0 - \bar{\mu}_1) - \frac{Db}{\rho^2} \left(\frac{B_0 + B_1}{B_1} \right) < 0, \quad (52)$$

where the inequality follows from (38).

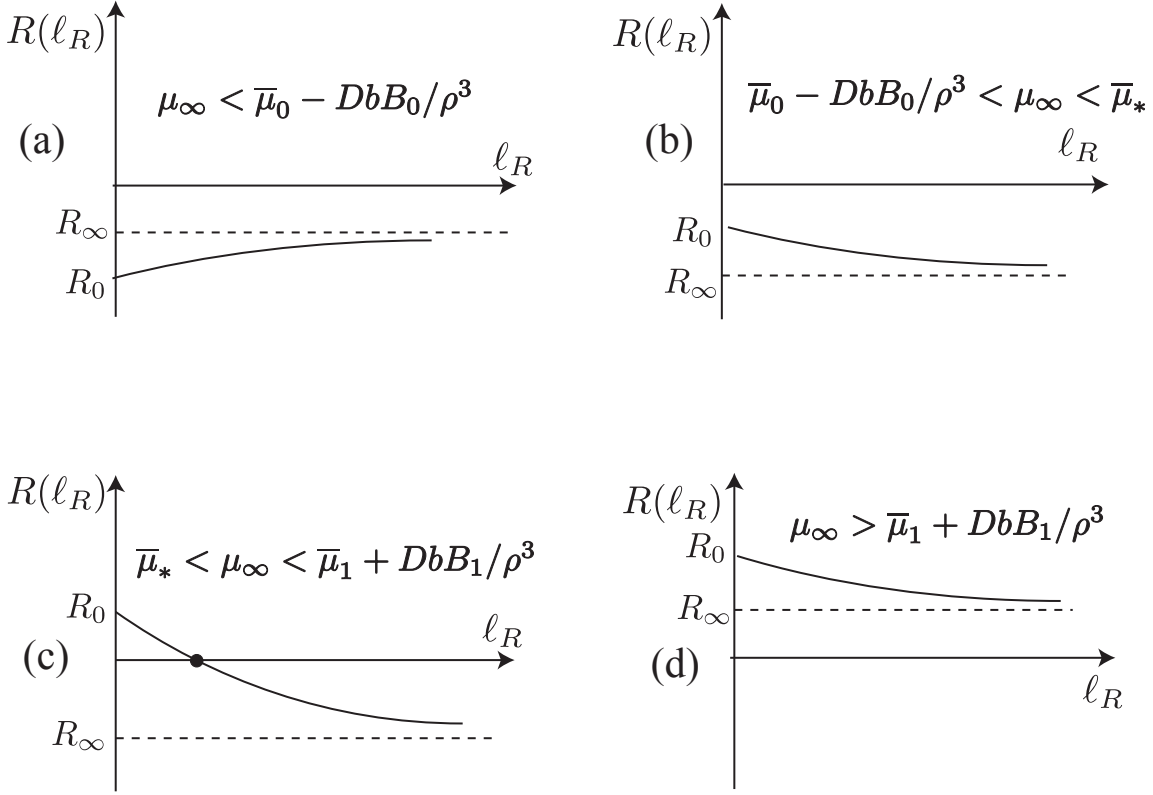


Figure 2: Graphs of $R(\ell_R)$ versus ℓ_R for different ranges of the remote chemical potential. The black dot in figure (c) corresponds to treading.

Note that in view of (38) and (41) the following ordering holds

$$\bar{\mu}_0 - DbB_0/\rho^3 < \bar{\mu}_0 < \bar{\mu}_* < \bar{\mu}_1 < \bar{\mu}_1 + DbB_1/\rho^3. \quad (53)$$

Case 1: $R(0) < R(\infty)$. In view of (47) this case occurs when

$$\mu_\infty < \bar{\mu}_0 - DbB_0/\rho^3. \quad (54)$$

The value of the function $R(\ell_R)$ increases monotonically from $R(0)$ to $R(\infty)$. It is readily seen that

$$R(\infty) \stackrel{(47)}{=} \frac{\rho}{B_1} [\mu_\infty - \bar{\mu}_1 - DbB_1/\rho^3] \stackrel{(54)}{<} \frac{\rho}{B_1} [\bar{\mu}_0 - \bar{\mu}_1 - DbB_0/\rho^3 - DbB_1/\rho^3] < 0, \quad (55)$$

since $\bar{\mu}_0 < \bar{\mu}_1$. Thus in this case one has $R(0) < R(\infty) < 0$ and so on the $\ell_R, \dot{\ell}_R$ -plane, the curve $\dot{\ell}_R = R(\ell_R)$ lies below the horizontal axis as depicted in Figure 6(a). Thus $\dot{\ell}_R < 0$ at all ℓ_R and so as time increases, the body shrinks and eventually disappears.

Case 2a: $0 > R(0) > R(\infty)$. In view of (47) this case corresponds to

90414-eq52}

$$\bar{\mu}_0 - DbB_0/\rho^3 < \mu_\infty < \bar{\mu}_*. \quad (56)$$

The value of the function $R(\ell_R)$ decreases monotonically from the negative value $R(0)$ to the value $R(\infty)$. Thus the graph of $\dot{\ell}_R = R(\ell_R)$ on the $\ell_R, \dot{\ell}_R$ -plane lies below the horizontal axis as depicted in Figure 6(b). Thus $\dot{\ell}_R < 0$ at all ℓ_R , and so as time increases, the body shrinks and eventually disappears.

Case 2b: $R(0) > 0 > R(\infty)$. In view of (47) this case corresponds to

90414-eq50}

$$\bar{\mu}_* < \mu_\infty < \bar{\mu}_1 + DbB_1/\rho^3, \quad (57)$$

where $\bar{\mu}_*$ was defined in (41). The function $R(\ell_R)$ decreases monotonically from the positive value $R(0)$ to the negative value $R(\infty)$. Thus the curve $\dot{\ell}_R = R(\ell_R)$ on the $\ell_R, \dot{\ell}_R$ -plane declines monotonically and intersects the horizontal axis at a unique point as depicted in Figure 6(c).

The intersection point shown by the black dot corresponds to a configuration called *treadmilling* at which $\dot{\ell}_R = 0$. The corresponding treadmilling length of the body, say ℓ_{TM} , is given by the root of the equation $R(\ell_{TM}) = 0$ and will be discussed further in Section 0.8.

Clearly, the initial-value problem

$$\dot{\ell}_R(t) = R(\ell_R(t)) \quad \text{for } t \geq 0, \quad \ell_R(0) = \ell_{TM},$$

has the unique stationary solution $\ell_R(t) = \ell_{TM}$ for $t \geq 0$. Since the slope of the curve $\dot{\ell}_R = R(\ell_R)$ is negative at the point $(\ell_{TM}, 0)$ where it crosses the horizontal axis (see Figure 6(c)), the treadmilling configuration is *stable*. To see this, suppose $\ell_R(0) > \ell_{TM}$. We see from Figure 6(c) that $\dot{\ell}_R < 0$ and so $\ell_R(t)$ will decrease with increasing time until it reaches the treadmilling length ℓ_{TM} (perhaps in infinite time). Likewise if $\ell_R(0) < \ell_{TM}$, we see from Figure 6(c) that $\dot{\ell}_R > 0$ and so $\ell_R(t)$ will increase with increasing time until it eventually reaches the treadmilling length ℓ_{TM} .

If, at the initial instant, the body has some other length, it will evolve monotonically towards ℓ_{TM} .

Case 2c: $R(0) > R(\infty) > 0$. In view of (47) this case corresponds to

90414-eq51}

$$\mu_\infty > \bar{\mu}_1 + DbB_1/\rho^3. \quad (58)$$

The function $R(\ell_R)$ decreases monotonically from the value $R(0)$ to the positive value $R(\infty)$. Thus the curve $\dot{\ell}_R = R(\ell_R)$ on the $\ell_R, \dot{\ell}_R$ -plane lies above the horizontal axis as depicted in Figure 6(d). Thus $\dot{\ell}_R > 0$ for all ℓ_R and so the body grows indefinitely.

These results are summarized in Table 2 and shown graphically in Figure 3.

Table 1: Growth of the body for various ranges of values of the remote chemical potential.

| Case | Chemical potential range | Evolution of the size $\ell_R(t)$ of the referential body |
|---------|---|--|
| Case 1 | $\mu_\infty < \bar{\mu}_0 - DbB_0/\rho^3$ | $\dot{\ell}_R(t) < 0$ Body shrinks and eventually disappears |
| Case 2a | $\bar{\mu}_0 - DbB_0/\rho^3 < \mu_\infty < \bar{\mu}_*$ | $\dot{\ell}_R(t) < 0$ Body shrinks and eventually disappears |
| Case 2b | $\bar{\mu}_* < \mu_\infty < \bar{\mu}_1 + DbB_1/\rho^3$ | $\dot{\ell}_R(t) \rightarrow 0$ Body converges to stable treading state |
| Case 2c | $\mu_\infty > \bar{\mu}_1 + DbB_1/\rho^3$ | $\dot{\ell}_R(t) > 0$ Body grows indefinitely |

14-table2}

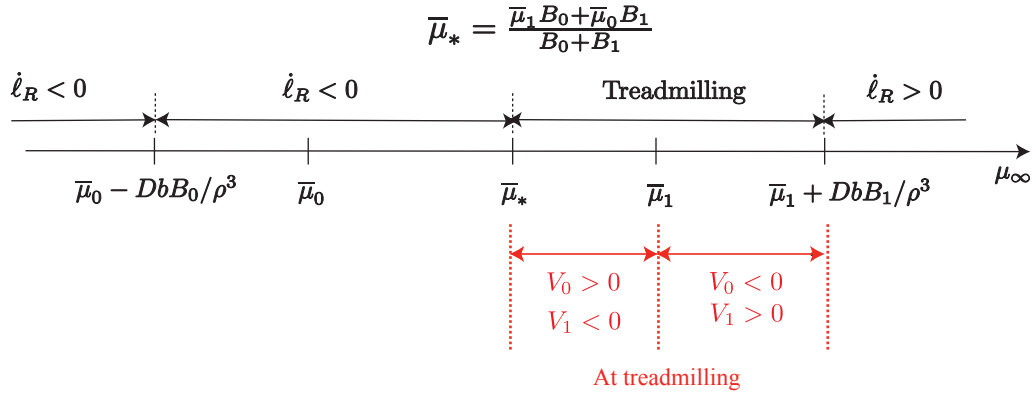


Figure 3: Growth of the length of the body. For small values of the solvent chemical potential, $\mu_\infty < \bar{\mu}_*$, the length of the body creases at all ℓ_R and so the solid eventually disappears. For large values of the solvent chemical potential, $\mu_\infty > \bar{\mu}_1 + DbB_1/\rho^3$, the length of the body increases at all ℓ_R and so the solid grows without bound. For intermediate values of the solvent chemical potential, $\bar{\mu}_* < \mu_\infty < \bar{\mu}_1 + DbB_1/\rho^3$, the body is attracted to a treading state $\dot{\ell}_R \rightarrow 0$ at some finite value of $\ell_R = \ell_{TM}$. *At the treading state*, within the treading range, in the sub-range $\bar{\mu}_* < \mu_\infty < \bar{\mu}_1$, association occurs at x_0 and dissociation occurs at x_1 ($V_0 > 0, V_1 < 0$), whereas in the sub-range $\bar{\mu}_1 < \mu_\infty < \bar{\mu}_1 + DbB_1/\rho^3$, dissociation occurs at x_0 and association occurs at x_1 ($V_0 < 0, V_1 > 0$).

0414-fig2}

0.8 Treadmilling:

Treadmilling refers to a process during which the length of the body in the current configuration does not change, i.e. $\dot{\ell}(t) = 0$ for all t . Since $\overset{*}{W}' > 0$ by (6), it follows from (25) that during a treadmilling process $\dot{\ell}_R(t) = 0$, and by (15) that $\dot{x}_1(t) = \dot{x}_0(t)$, and in turn by (39) that $V_1(t) = -V_0(t)$. Thus

$$\text{Treadmilling : } \dot{\ell}(t) = 0 \Leftrightarrow \dot{\ell}_R(t) = 0 \Leftrightarrow \dot{x}_1(t) = \dot{x}_0(t) \Leftrightarrow V_1(t) = -V_0(t). \quad (59)$$

Note from the last equality that though the length of the body does not change during treadmilling, $\ell(t) = \text{constant}$, the growth rates at the two ends of the body need not vanish: it is only necessary that the rate of association at one end equal the rate of dissociation at the other end, $V_1(t) = -V_0(t) \neq 0$, and not that they must each vanish individually.

In view of (46), the referential length of the body at treadmilling, $\ell_R = \ell_{\text{TM}}$, given by

$$R(\ell_R) \Big|_{\ell_R = \ell_{\text{TM}}} = 0, \quad (60)$$

is the unique positive root ℓ_{TM} of the equation

$$-\overset{*}{W}(-b\ell_{\text{TM}}) = \frac{Db(B_0 + B_1)}{\rho^2} \frac{\mu_\infty - \bar{\mu}_*}{\bar{\mu}_1 + DbB_1/\rho^3 - \mu_\infty}. \quad (61)$$

That this equation has a unique positive root when the chemical potential lies in the treadmilling range $\bar{\mu}_* < \mu_\infty < \bar{\mu}_1 + DbB_1/\rho^3$ (and not otherwise) follows from the monotonicity of the right-hand side of (61) with respect to μ_∞ and the properties of $\overset{*}{W}$. The treadmilling length ℓ_{TM} is a function of the remote chemical potential μ_∞ : $\ell_{\text{TM}}(\mu_\infty)$. In fact, it is readily seen to be a monotonically increasing function of μ_∞ , with $\mu_\infty \rightarrow \bar{\mu}_*$ when $\ell_{\text{TM}} \rightarrow 0$ and $\mu_\infty \rightarrow \bar{\mu}_1 + DbB_1/\rho^3$ when $\ell_{\text{TM}} \rightarrow \infty$. The bold curve \mathcal{C}_{TM} in Figure 4 is a plot of $\ell_R = \ell_{\text{TM}}(\mu_\infty)$ on the μ_∞, ℓ_R -plane.

The solution of the initial-value problem $\dot{\ell}_R(t) = R(\ell_R(t)), t \geq 0$ for any given value of $\ell_R(0)$ evolves as shown in Figure 4. Based on the results summarized in Table 1, the solution evolves towards the horizontal axis ($\ell_R(t) \rightarrow 0$) when the value of the remote chemical potential lies in the range $0 < \mu_\infty \leq \bar{\mu}_*$. It evolves away from the horizontal axis ($\ell_R(t) \rightarrow \infty$) when the value of the chemical potential lies in the range $\mu_\infty \geq \bar{\mu}_1 + DbB_1/\rho^3$. For intermediate values of the chemical potential, $\bar{\mu}_* \leq \mu_\infty \leq \bar{\mu}_1 + DbB_1/\rho^3$, the solution is attracted to the treadmilling solution ($\ell_R(t) \rightarrow \ell_{\text{TM}}$) corresponding to the curve \mathcal{C}_{TM} in Figure 4.

At treadmilling we have $V_0 = -V_1$, see (59). It is possible that either $V_0 > 0$ and $V_1 < 0$ corresponding to association at x_0 and dissociation at x_1 or, $V_0 < 0$ and $V_1 > 0$ corresponding

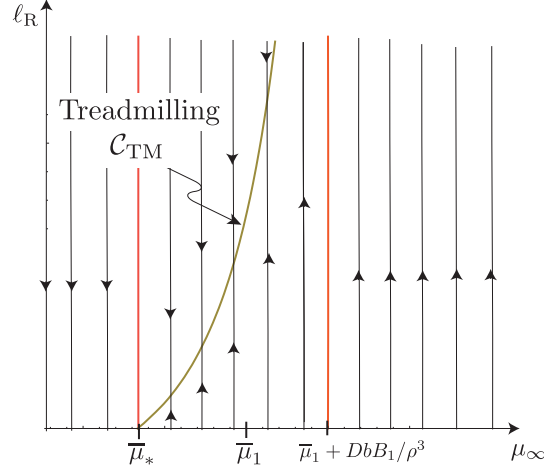


Figure 4: Sense in which ℓ_R evolves at different values of the remote chemical potential. For large values of the remote chemical potential, $\mu_\infty > \bar{\mu}_1 + DbB_1/\rho^3$, the length of the body increases at all ℓ_R . For intermediate values of the chemical potential, $\bar{\mu}_* < \mu_\infty < \bar{\mu}_1 + DbB_1/\rho^3$, the body is attracted to a treadmilling state $\dot{\ell}_R \rightarrow 0$ and $\ell_R(t) \rightarrow \ell_{TM}$. Such states are associated with the curve \mathcal{C}_{TM} . For small values of the remote chemical potential, $0 < \mu_\infty < \bar{\mu}_*$, the length of the body length decreases at all ℓ_R .

to dissociation at x_0 and association at x_1 . We now discern as to which of these occurs, and under what conditions. Observe from (39)₂ and (45) that the growth rate $V_1 = \dot{x}_1$ obeys

$$V_1 < 0 \quad \text{for } \mu_\infty < \bar{\mu}_1, \quad V_1 > 0 \quad \text{for } \mu_\infty > \bar{\mu}_1. \quad (62)$$

Therefore at treadmilling, since $V_0 = -V_1$, it follows that

$$V_0 > 0 \quad \text{for } \mu_\infty < \bar{\mu}_1, \quad V_0 < 0 \quad \text{for } \mu_\infty > \bar{\mu}_1. \quad (63)$$

Therefore *during treadmilling*, when the value of the chemical potential lies in the range $\bar{\mu}_* < \mu_\infty < \bar{\mu}_1$, association occurs at x_0 and dissociation occurs at x_1 ($V_0 > 0, V_1 < 0$). For $\bar{\mu}_1 < \mu_\infty < \bar{\mu}_1 + DbB_1/\rho^3$, dissociation occurs at x_0 and association occurs at x_1 ($V_0 < 0, V_1 > 0$). This is shown in Figure 3.

0.9 Growth at each end.

We now look in more detail at the conditions under which each end of the body grows or shrinks. It follows from (43) that on the μ_∞, ℓ_R -plane, the curve \mathcal{C}_0 corresponding to $-V_0 = \dot{x}_0(\ell_R, \mu_\infty) = 0$ is described by

$$\mathcal{C}_0 : \quad \mu_\infty = \bar{\mu}_0 - \frac{1}{\rho} W^*(-b\ell_R) \quad (V_0 = 0). \quad (64)$$

This curve \mathcal{C}_0 is shown in Figure 5. Note that it rises monotonically from the point $\mu_\infty = \bar{\mu}_0, \ell_R = 0$ and goes off to infinity as $\mu_\infty \rightarrow \infty$. Points to the left of \mathcal{C}_0 correspond to $V_0 < 0$ and therefore to dissociation at x_0 . Points to the right of \mathcal{C}_0 correspond to $V_0 > 0$ and therefore to association at x_0 .

Similarly from (45), the curve \mathcal{C}_1 in the μ_∞, ℓ_R -plane corresponding to $V_1 = \dot{x}_1(\ell_R, \mu_\infty) = 0$ is the vertical straight line

$$\mathcal{C}_1: \quad \mu_\infty = \bar{\mu}_1 \quad (V_1 = 0). \quad (65)$$

Points to the left of \mathcal{C}_1 correspond to $V_1 < 0$ and therefore to dissociation at x_1 . Points to the right of \mathcal{C}_1 correspond to $V_1 > 0$ and therefore to association at x_1 . These are labelled in Figure 5.

It can be readily shown from (61), (64) and (65) that the treadmilling curve \mathcal{C}_{TM} in Figure (4) intersects both curves \mathcal{C}_0 and \mathcal{C}_1 in Figure 5 at $\mu_\infty = \bar{\mu}_1$. This is shown in Figure 6. (Nominally \mathcal{C}_0 also intersects \mathcal{C}_{TM} at $\mu_\infty = \bar{\mu}_0 - DbB_0/\rho^3$ but this is outside the domain of \mathcal{C}_{TM} .) For $\bar{\mu}_* < \mu_\infty < \bar{\mu}_1$ the curve \mathcal{C}_{TM} lies below the curve \mathcal{C}_0 , and for $\bar{\mu}_1 < \mu_\infty < \bar{\mu}_1 + DbB_1/\rho^3$ the curve \mathcal{C}_{TM} lies above \mathcal{C}_0 . It follows that *on the curve* \mathcal{C}_{TM} one has $V_0 > 0, V_1 < 0$ for $\bar{\mu}_* < \mu_\infty < \bar{\mu}_1$ and $V_1 > 0, V_0 < 0$ for $\bar{\mu}_1 < \mu_\infty < \bar{\mu}_1 + DbB_1/\rho^3$ (as already seen at the end of Section 0.8).

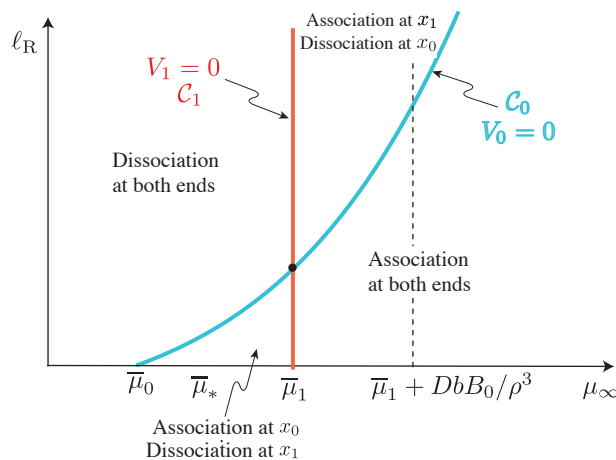


Figure 5: Association at x_0 and x_1 corresponds to $V_0 > 0$ and $V_1 > 0$ respectively; dissociation at x_0 and x_1 corresponds to $V_0 < 0$ and $V_1 < 0$ respectively;

0.10 Parameters

The parameters involved in the model, and their dimensions, are listed in Table 2. Consider the velocities v_{k0} and v_{k1} associated with the growth kinetics at x_0 and x_1 and the velocity

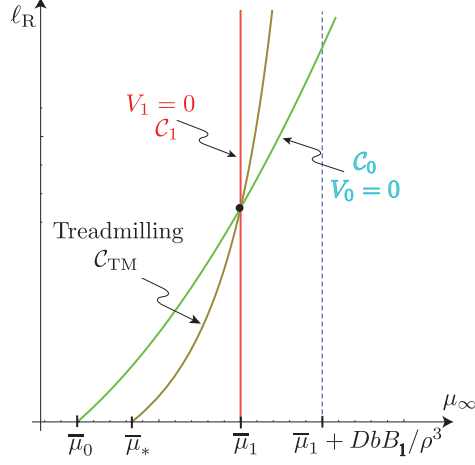


Figure 6: Curves \mathcal{C}_{TM} , \mathcal{C}_0 and \mathcal{C}_1 .

90414-fig5}

v_d associated with diffusion:

$$v_{k0} = \frac{\rho\bar{\mu}_0}{B_0}, \quad v_{k1} = \frac{\rho\bar{\mu}_1}{B_1}, \quad v_d = \frac{Db}{\rho^2}. \quad (66)$$

The problem involves the following non-dimensional parameters:

$$\frac{E}{\rho\bar{\mu}_0}, \quad c_0 = \frac{v_d}{v_{k0}} = \frac{DbB_0}{\rho^3\bar{\mu}_0}, \quad c_1 = \frac{v_d}{v_{k1}} = \frac{DbB_1}{\rho^3\bar{\mu}_1}, \quad M = \frac{\bar{\mu}_1}{\bar{\mu}_0}, \quad \varepsilon = \frac{E}{\rho\bar{\mu}_0}. \quad (67)$$

The nondimensional size of the body is $b\ell_R/E$ and the nondimensional remote chemical potential is $\mu_\infty/\bar{\mu}_0$.

Figures 4, 5 and 6 are drawn with these parameters having the values

$$c_0 = 0.5, \quad c_1 = 0.5, \quad M = 2, \quad \varepsilon = 1. \quad (68)$$

The complementary energy function \bar{W}^* was taken to be that given in (14).

Table 2: Parameters in the model.

| | | |
|----------------------------|--|----------------------------------|
| ρ | mass density | mass/volume |
| b | body force due to drag | stress/length |
| E | elastic modulus | energy/volume |
| D | diffusion coefficient | mass times time per unit volume |
| $\bar{\mu}_1, \bar{\mu}_1$ | chemical potential of bound monomers | energy/mass |
| μ_∞ | chemical potential of surrounding monomer solution | energy/mass |
| B_0, B_1 | kinetic coefficients in growth laws | mass per unit area per unit time |

14-table1}